Struct Chem (2017) 28:925–943
DOI 10.1007/s11224-016-0895-6

ORIGINAL RESEARCH

Intramolecular single H bonding vs bifurcation in tuning the conformation of 2,2′-dihydroxybenzophenone and its derivatives: a DFT insight

Demeter Tzeli[1] · **Petros G. Tsoungas**[2] · **Ioannis D. Petsalakis**[1] · **Paweł Kozielewicz**[3]

Received: 13 October 2016 / Accepted: 29 November 2016 / Published online: 15 December 2016

Abstract 2,2′-dihydroxybenzophenones and their oxime and N-acyl hydrazone derivatives have been studied via the DFT/B3LYP-6-311++G** methodology. An almost coplanar bifurcated six-membered H bridge is found in ketones. A similar H bridge, accompanied by a seven-membered one in oximes and a nine-membered-like one in hydrazones, is also formed. While the closed (two pseudo rings) conformer is the lowest energy one in 2,2′-dihydroxybenzophenones and their oximes, the semi-closed conformer (one pseudo ring) corresponds to the lowest energy one in N-acyl hydrazones. The ΔH_f of the closed conformer compared to its open counterpart is ca. 17 kcal/mol in 2,2′-dihydroxybenzophenones while that in oximes is ca. 11 kcal/mol. The energy barrier in changing from the closed to the open (no pseudo ring) conformation is <3 kcal/mol for all 2,2′-dihydroxybenzophenones and their oximes. The impact of intramolecular hydrogen bonding on the variation of ΔH_f of the conformers are discussed with respect to mono- and di-*p*-substitution of 2,2′-dihydroxybenzophenone structure as well as to its conversion into oxime and hydrazone derivatives. ΔH_f of both closed and semi-closed conformers decreases, throughout the series, unlike that of semi-closed conformer of the Br-substituted ones. A slightly decreased enthalpy due to intramolecular hydrogen bonding in 2,2′-dihydroxybenzophenones is attributed to *p*-substitution and a further significant decrease is noted in going from 2,2′-dihydroxybenzophenones to oximes. An enthalpy increase, on the other hand, occurs in moving from oxime to hydrazone, again with the exception of semi-closed conformer of the Br-substituted conformers.

Keywords 2,2′-dihydroxybenzophenones · Oxime · N-acyl hydrazone · Intramolecular H bonding · Bifurcation · Calculations · DFT

Electronic supplementary material The online version of this article (doi:10.1007/s11224-016-0895-6) contains supplementary material, which is available to authorized users.

✉ Demeter Tzeli
dtzeli@eie.gr

✉ Petros G. Tsoungas
pgt@pasteur.gr

[1] Theoretical and Physical Chemistry Institute, National Hellenic Research Foundation, 48 Vassileos Constantinou Ave, 116 35 Athens, Greece

[2] Department of Biochemistry, Hellenic Pasteur Institute, 127 Vas. Sofias Ave, GR-11521 Athens, Greece

[3] School of Clinical and Experimental Medicine, College of Medical and Dental Sciences, University of Birmingham, Edgbaston, Birmingham B15 2TT, UK

Introduction

Hydroxybenzophenones exhibit interesting photophysical [1], photochemical [2] and biological properties [3]. They have a wide range of applications, e.g. in laser dyes [4], as polymer stabilizers [5], biologically active metabolites [6] or in sunscreens [7, 8] to name a few [9]. They are absorbed through the human skin, therefore, bioaccumulation may occur in wildlife and humans [10]. It is known that their reactivity and their biological activity are linked to their acid-base and metal chelating properties [11]. Their pharmacology usually works through direct interaction with metal-bearing active enzyme sites [12]. Their oximes [13, 14] and hydrazones [15, 16] have been tested for a broad range of biological activities and a few hydrazones have been found to display anti-inflammatory activity [16, 17]. Their molecular structure and

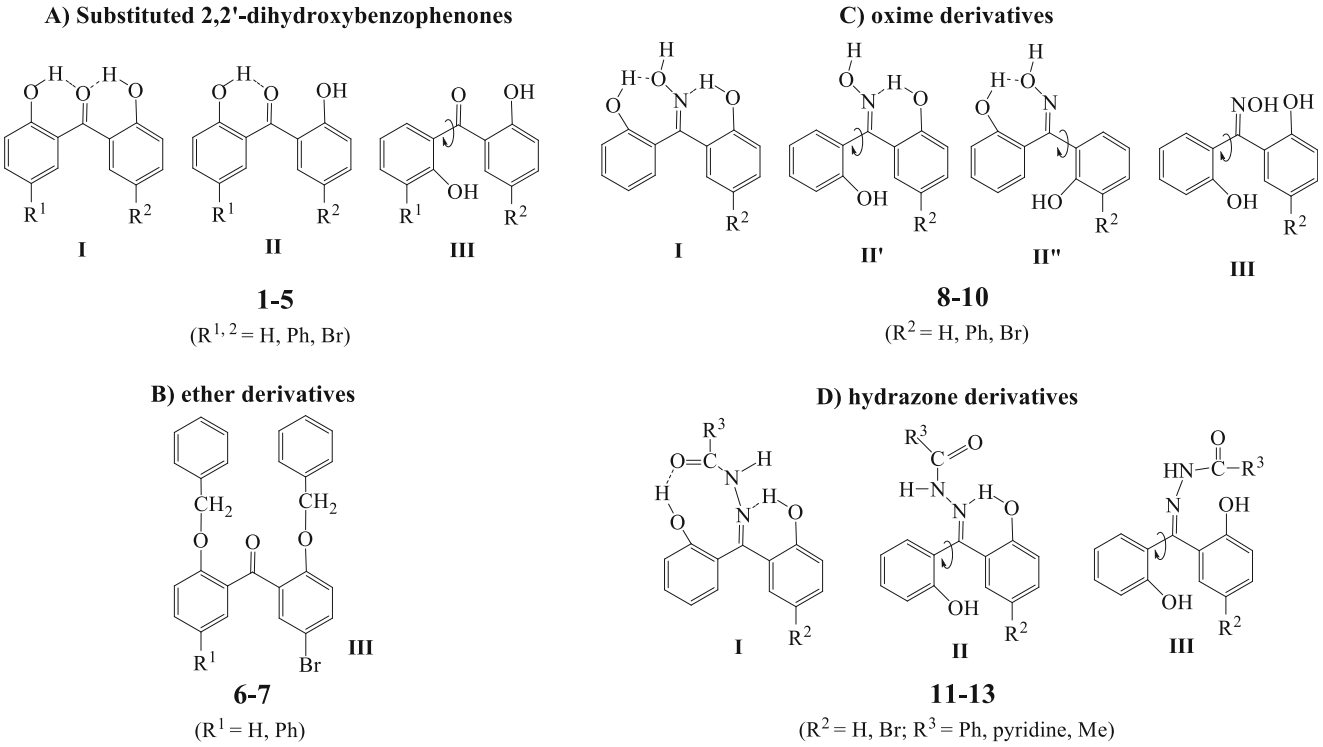

Chart 1 Compounds **1**–**13**. Pseudo ring conformations: type **I** (bifurcated, closed form), type **II** (singly H-bonded conformation, semi-closed form) and type **III** (non H-bonded conformation, open form)

inherent intramolecular H bonding have been studied via theoretical methods [18, 19].

Much attention has been directed towards deciphering the nature of the bonding in low-barrier short hydrogen bonds [18–25]. Gilli et al. have proposed the resonance-assisted hydrogen bonding (RAHB) model to account for the very short O-H···O and N-H···O distances observed in conjugated neutral systems containing H bonds [26]. RAHBs are present in many biological processes, which makes them an important topic in fields such as enzyme catalysis [25, 27], organocatalysis [25], (bio)chemistry and molecular biology [28]. Studies have focused mostly on H bonds that involve a single donor-acceptor

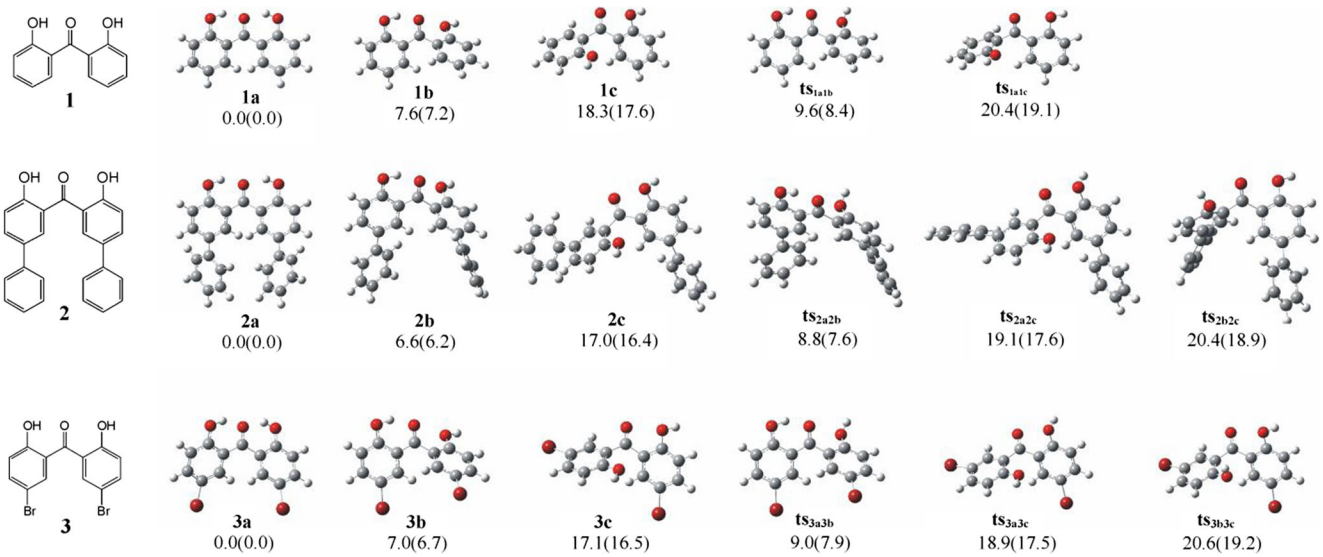

Fig. 1 Minima conformers and transition states (ts) of **1**, **2**, and **3**. The relative energies (relative enthalpies at 298.150 K and 1 Atm) in kcal/mol are given (C atoms are indicated by *grey spheres*, H by *white*, O by *red*, N by *blue*, and Br by *dark red*)

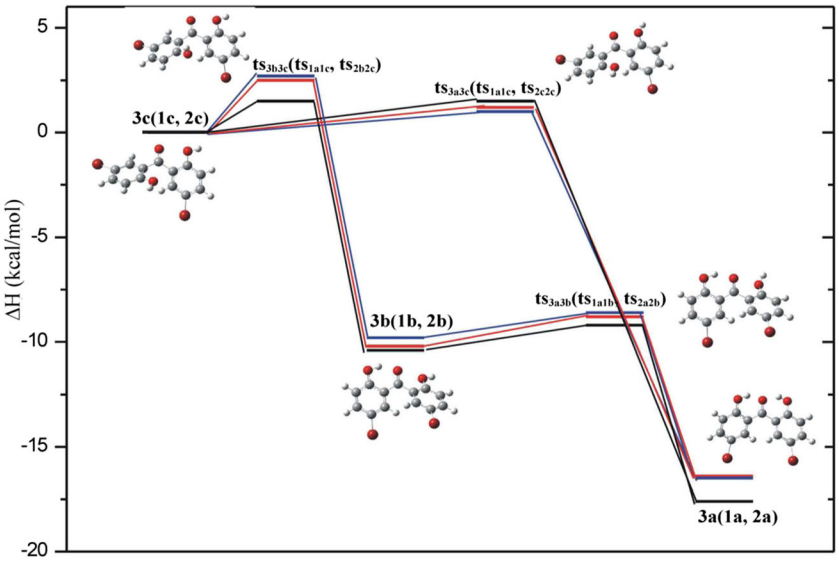

Fig. 2 Reaction enthalpy (298.150 K; 1 Atm) for the conformational isomerization of the open structure (type **III**) of **1**, **2**, and **3** to the closed structure (type **I**). *Black lines* correspond to **1**, *red lines* to **2** and *blue lines* to **3**, see Fig. 1. Only the conformers and transition states of **3** are given for simplicity (C atoms are indicated by *grey spheres*, H by *white*, O by *red*, and Br by *dark red*)

pair. However, there are instances in which the H bonding pattern may include more than one donor or acceptor [25]. Such bonds, known as bifurcated H bonds, describe the interaction between one donor to two acceptors (e.g., C=O···H···O=C) or its alternative variation, i.e., two donors to a single acceptor (e.g., N-H···O···H-N). Such bonding interactions are said to be overcoordinated. The prevalence of such bifurcated H bonds in proteins has been analysed [23] and has even been implicated in bending of helices [29, 30].

2,2′-Dihydroxybenzophenones [31, 32] and derivatives exhibit obvious structure similarities to their mono-hydroxy analogues. An important application in both chemistry and biology is their use in axial and helical chirality [33]. They have also been found as potent inhibitors against hGSTA1-1 involved in multiple drug resistance [34]. Recently diverse routes for their synthesis have been described and their structure profile has been scrutinized by DFT/B3LYP-6-311++G** methodology and NMR spectroscopy [32]. Significant anti-inflammatory activity, mainly of their oxime and hydrazone derivatives, has been found, competing that of marketed drugs. In silico docking studies point to the perspective potency of these structures as COX-1/COX-2 inhibitors [32]. The significance of these results provided the impetus to explore the geometrical features of their conformers and requirements for their interconversion, thus, profiling likely pathways for their displayed biological activity.

Oximes and N-acylhydrazones of 2,2′-dihydroxy benzophenones have been chosen to elucidate the impact of (a) intramolecular H bonding (IHB) on the relative stability and interconversion of the various conformers, its competition between single or bifurcated formations and (b) IHB variations from steric constraints triggered by *p*-substitution. To that end, transition states of interconversion, H bond strengths and relative stabilities of the conformers have been calculated by DFT calculations.

Computational details

Compounds **1**–**13** (Chart 1) have been studied. Three to twelve low energy minima structures were calculated for each one of them. These minima are divided into three categories: (a) the "bifurcated" or closed form (type **I**), i.e., the structures with two intramolecular H-bonded pseudo (quasi) 6-, 7- or 9-membered rings, (b) the singly H-bonded or semi-closed form (type **II**), i.e., the structures with one intramolecular H-bonded pseudo ring, and (c) the non H-bonded structures or open form (type **III**), i.e., the structures with no intramolecular H-bonded pseudo rings (Chart 1). It should be noted that the closed or "bifurcated" form, i.e., two donors to a single acceptor (e.g., -O-H···O···H-O-) is found only in ketones **1**–**5** (Chart 1A). Transition states have been calculated for the interconversion of conformers among **I**, **II** and **III** types, as well as for those with multiple **I**-**III** types.

All minima and transition states for the conformers of **1**–**13** were fully optimized. The pathways for the transition between the various conformers of the molecules were calculated. The calculations were carried out using the hybrid B3LYP functional [35, 36] coupled with the 6-311G++(d,p) [37]. The suitability of the B3LYP functional has been tested in many cases and has been found reliable for theoretical calculations [38–41] and prediction of organic reaction mechanisms [42,

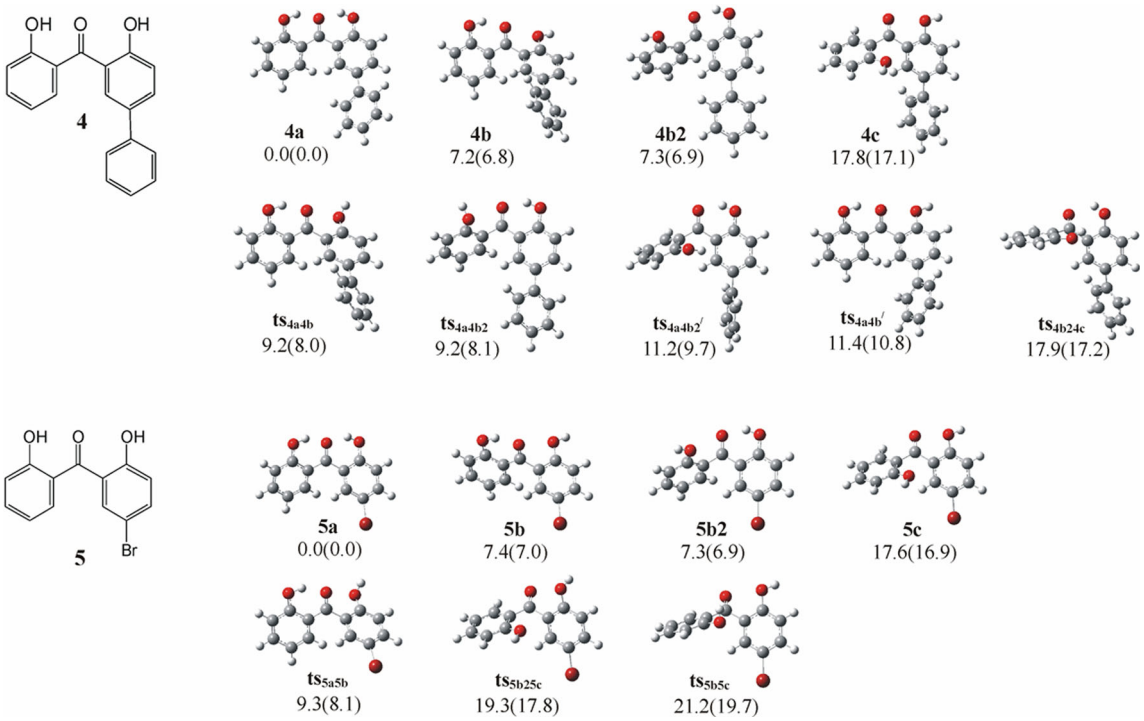

Fig. 3 Minima and transition states (ts) of **4** and **5**. The relative energies (relative enthalpies at 298.150 K; 1 Atm) in kcal/mol are given (C atoms are indicated by *grey spheres*, H by *white*, O by red, and N by *blue*, and Br by *dark red*)

43]. For example in similar compounds with the ones calculated here [43] the credibility of the B3LYP functional was tested for the calculated minima, transition states and tentative reaction pathways using the M06-2X functional and the second order Møller-Plesset perturbation theory (MP2) in conjunction with the 6-311G+(d,p) and aug-cc-pVTZ basis sets. B3LYP/6-311G+(d,p) was found to be a good choice [43].

For all structures, the vibrational frequencies were calculated to confirm that the structures are true conformers or transition states. Their relative and zero point energies, corrected values, relative thermal energies, enthalpies, free energies, dipole moments and cartesian coordinates are given in the Supporting Information (SI). All computations have been carried out and visualized using Gaussian 09 program [44].

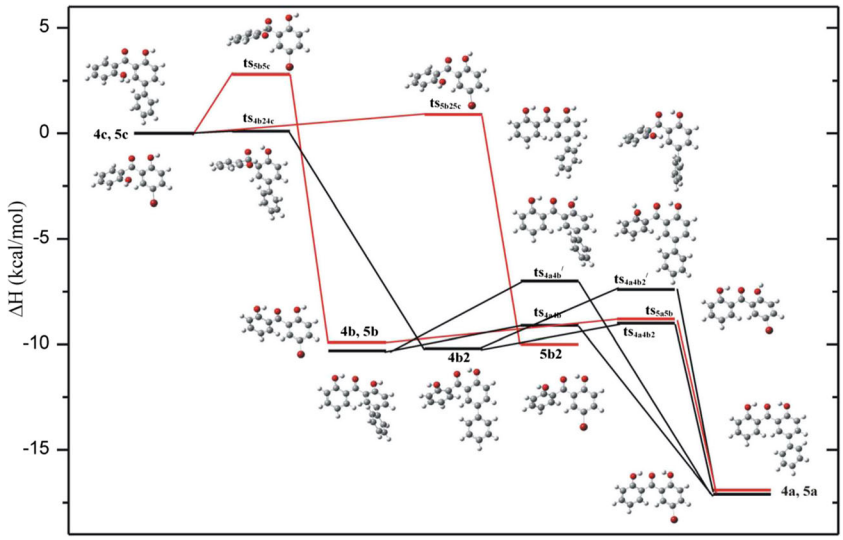

Fig. 4 Reaction enthalpy (298.150 K; 1 Atm) for the conformational isomerization of the open structure (type **III**) of **4** and **5** to the closed structure (type **I**). *Black lines* correspond to **4** (see Fig. 3) and *red lines* to **5** (see Fig. 3) (C atoms are indicated by *grey spheres*, H by *white*, O by *red*, N by *blue*, and Br by *dark red*)

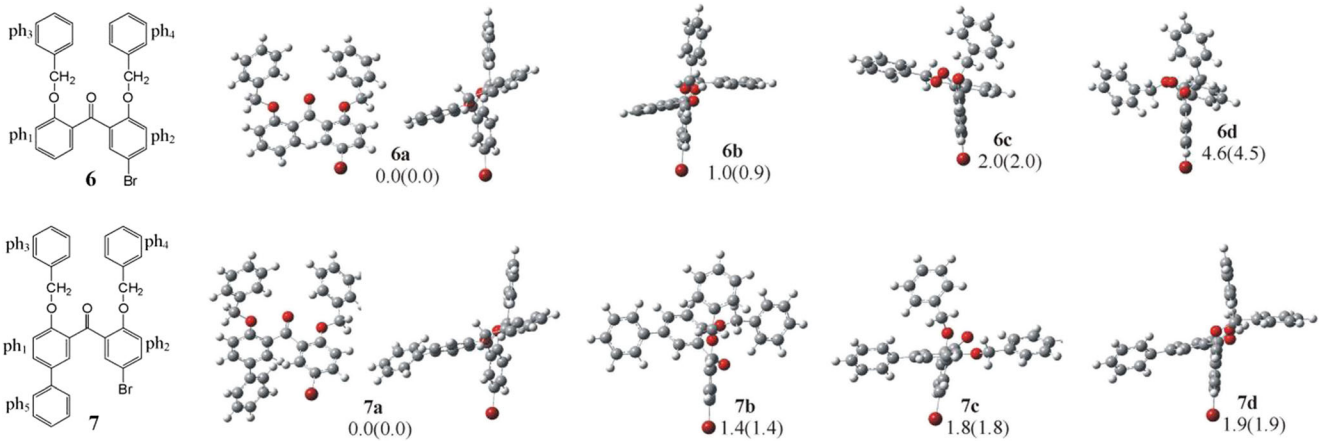

Fig. 5 Minima conformers of **6** and **7**. The relative energies (relative enthalpies at 298.150 K; 1 Atm) in kcal/mol are given. The lowest **a** minima are given from two different perspectives

Results and discussion

2,2′-dihydroxybenzophenones

The >C=O and the phenol hydroxyl groups build up non equivalent RAHB-stabilized [45] IHB interactions, leading to non planar conformations. The latter, however and the resulting distortion cannot impede bifurcation in **1**–**5**.

1, **2**, and **3:** Minima and transition states (ts) are depicted and relative enthalpies are given for their conformers in Fig. 1. Their reaction enthalpy changes during the conformational isomerization of type **III** (open form) to type **I** (closed form) is depicted in Fig. 2. Enthalpy barriers for the conversion of **c** (type **III**) to **b** (semi-closed form, type **II**) in **1**–**3** are only 1.5, 2.5 and 2.7 kcal/mol, the lowest one of which is expectedly observed for **1**. The slightly higher values are attributed to steric constraints due to *p*-substitution in **2** and **3**. Still lower enthalpy barriers of 1.2, 1.4 and 1.2 kcal/mol are found for the isomerization of **b** to **a** (type **I**) for **1**, **2**, and **3**, respectively. We observe that the enthalpy of **a** (closed form) in **1**–**3** is lower to that of **c** (open form) by 18.3(17.6), 17.0(16.4), and 17.1(16.5) kcal/mol, respectively. For the parent **1**, lacking any substitution constraints, the stabilization of the **a** form is slightly more demanding than that of the **c** form by ca. 1 kcal/mol.

Intramolecular H bond distances, O-H…O angles (φ) of the pseudo 6-rings and dihedral angles (d) of the **a** form in **1**, **2**, and **3** (Table 1S, SI). No variation for the H bond distances and angles φ and a marginal one for the dihedral angle (d) have been observed. The dihedral angle, engaging the two phenol groups, increases drastically from ca. 44 degrees in **a** (closed form), to ca. 70 degrees in **b** (semi-closed form) up to ca. 108 degrees in **c** (open form) in agreement with experimental data for similar compounds [46–48]. X-ray data of **1a** indicate a limited distortion with a dihedral angle at 38 degrees [46, 47] compared to a calculated value of 44 degrees. ^{1}H NMR chemical shifts are indicative of a bifurcated H bridge [32, 49]. *p*-Substitution leads to a varying dihedral angle of the two phenol groups) in the transition states of **1**–**3**. The two RAHB-stabilized pseudo 6-rings (HO…H) form a dihedral angle of ca. 20 degrees in all **a** conformers.

4 and **5:** The minima and transition states (ts) of **4** and **5** conformers are depicted in Fig. 3. These structures have only one of their phenol rings occupied by a phenyl or a Br substituent at the p-position, respectively. Relative enthalpies are given in Fig. 3 while the reaction enthalpy variation upon conformational isomerization of **c** (open form) of **4** and **5** to **a** (closed form) conformation is depicted in Fig. 4. Worth noting is that **b** and **b2** (semi-closed forms) can be differentiated through the orientation of the pseudo six-membered ring, e.g. adjacent to or away from the *p*-substituted phenyl group (Fig. 4). The enthalpy barrier for the isomerization of **c** (open form) to **b2** (semi-closed form) is less than 1 kcal/mol while that for the conversion to **b** is 3 kcal/mol, (Fig. 4). Moreover, the enthalpy barrier for the isomerization of **b** or **b2** (semi-closed form) to **a** (closed form) (two pseudo 6-rings formed through bifurcation) is only ca. 1.2 kcal/mol. Thus, it appears that the interconversion follows the **c** → **b2** → **a** pathway with an enthalpy requirement of ca. 1 kcal/mol (Fig. 4).

Looking at the interconversion process in ketones **1**–**5** it follows that (a) conversion of **c** to **b** has an enthalpy demand of less than 3 kcal/mol, (b) the largest enthalpy of ca. 18.3(17.6) kcal/mol is observed for the conformation changes in **1**, (c) there is a lower enthalpy barrier and a higher enthalpy toll for stabilization of ca. 0.5 kcal/mol for *p*-substitution on only one of the rings (**4** and **5**) as opposed to *p*-substitution on both rings (**2** and **3**), (d) the largest enthalpy barrier is observed for **3**, (e) the enthalpy barrier of the interconversion **b** to **a** in the series is ca. 1.2 kcal/mol, (f) the **a** conformer is more stable than the **c** one by ca. 17 kcal/mol.

Selected geometries of **a**, **b**, **b2**, and **c** minima and transition structures of **4** and **5** are given in Table 2S, SI. The intramolecular H bond distances and the O-H…O angles of their pseudo

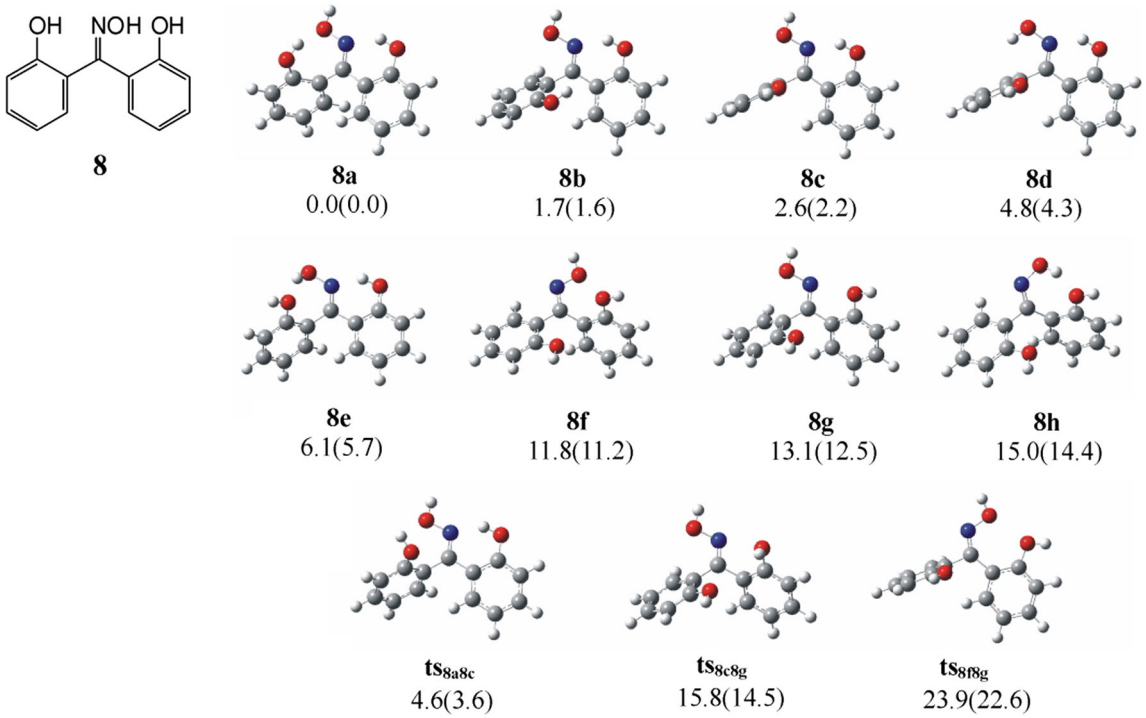

Fig. 6 Minima conformers and transition states (ts) of **8** . The relative energies (relative enthalpies at 298.150 K; 1 Atm) in kcal/mol are given (C atoms are indicated by *grey spheres*, H by *white*, O by *red*, and N by *blue*)

6-rings are in the range 1.69 to 1.74 Å and 144 to 147 degrees, respectively (Tables 1S and 2S, SI). Interestingly, a twisted six-membered ring in the $\mathbf{ts_{2a2c}}$ transition state, leads to a weak H…O interaction of 2.303 Å (Table 2S, SI). The dihedral angles of two pseudo six-membered rings (HO…H) of **a** are in the range 20–24 degrees while those of one pseudo six-membered ring (HO…H) adjacent to a phenyl group is ca. 5 degrees and ca. 15 degrees when two pseudo six-membered rings are formed. Of note is the dihedral angle engaging the two phenols, of 44 degrees, for the same conformer in **1**–**5**. ^{1}H NMR δ values for the mono-substituted **4** and **5** display two deshielded OH resonances, indicative of a bifurcated H bridge in the RAHB

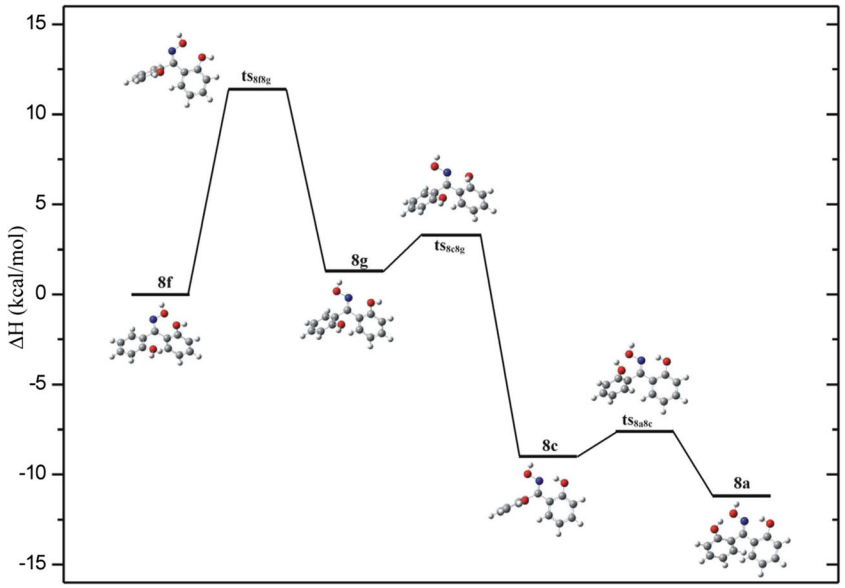

Fig. 7 Reaction enthalpy (298.150 K; 1 Atm) for the conformational isomerization of the open form (type **III**) of **8** to the closed form (type **I**) (C atoms are indicated by *grey spheres*, H by *white*, O by *red*, and N by *blue*)

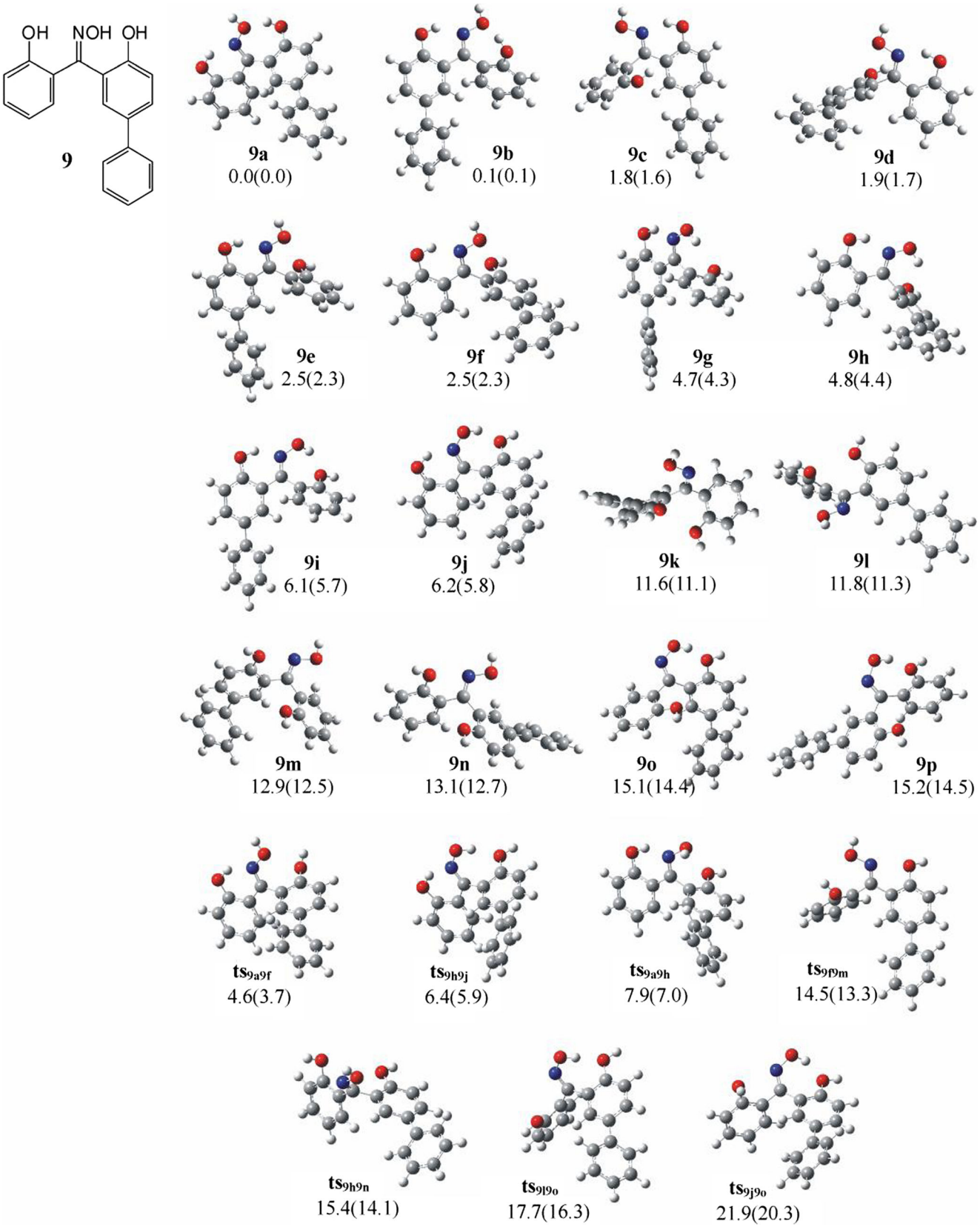

Fig. 8 Minima and transition states (ts) of **9**. The relative energies (relative enthalpies at 298.150 K; 1 Atm) in kcal/mol are given (C atoms are indicated by *grey spheres*, H by *white*, O by *red*, and N by *blue*)

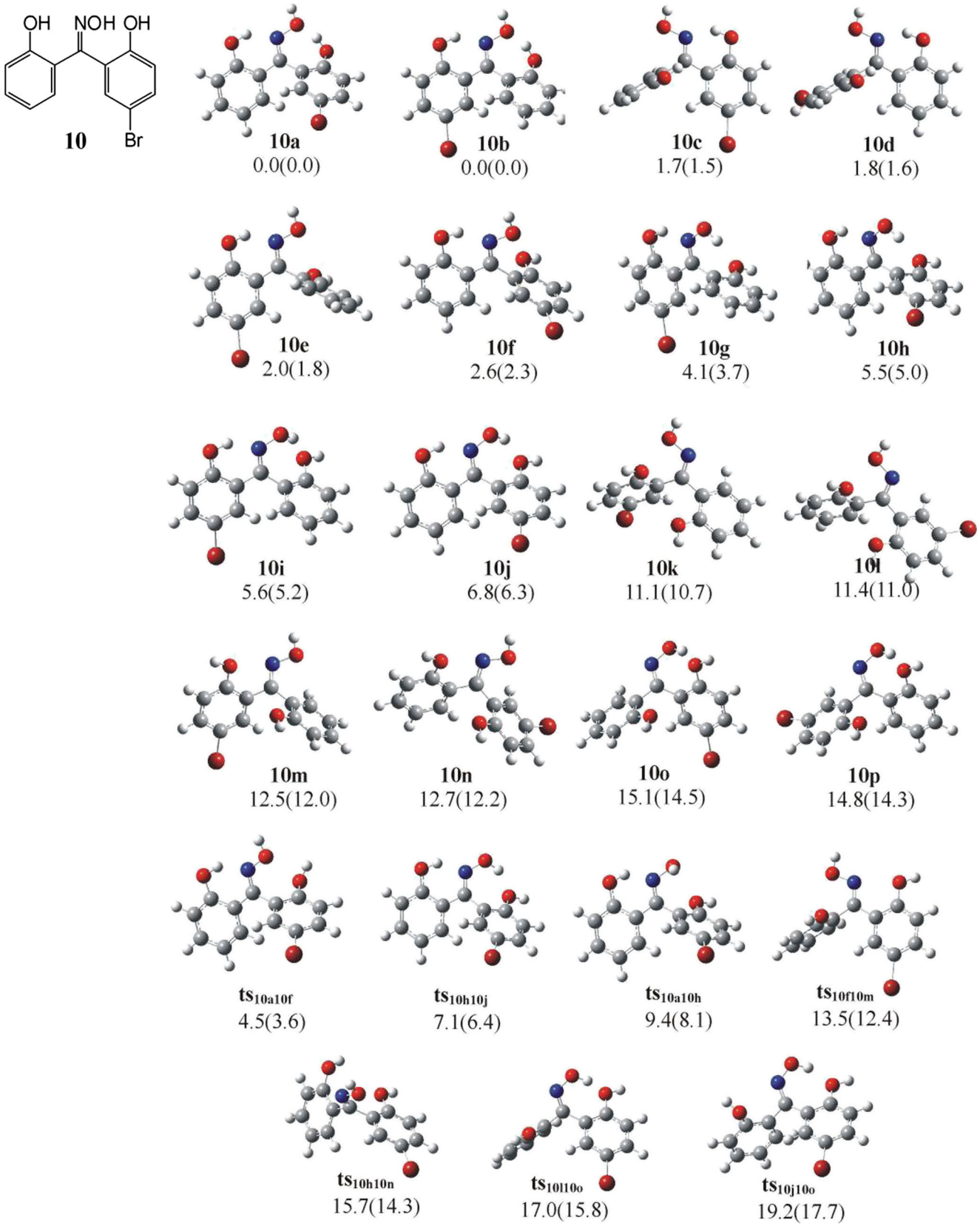

Fig. 9 Minima and transition states (ts) of **10**. The relative energies (relative enthalpies at 298.150 K and 1 Atm) in kcal/mol are given. (C atoms are indicated by *grey spheres*, H by *white*, O by *red*, N by *blue*, and Br by *dark red*)

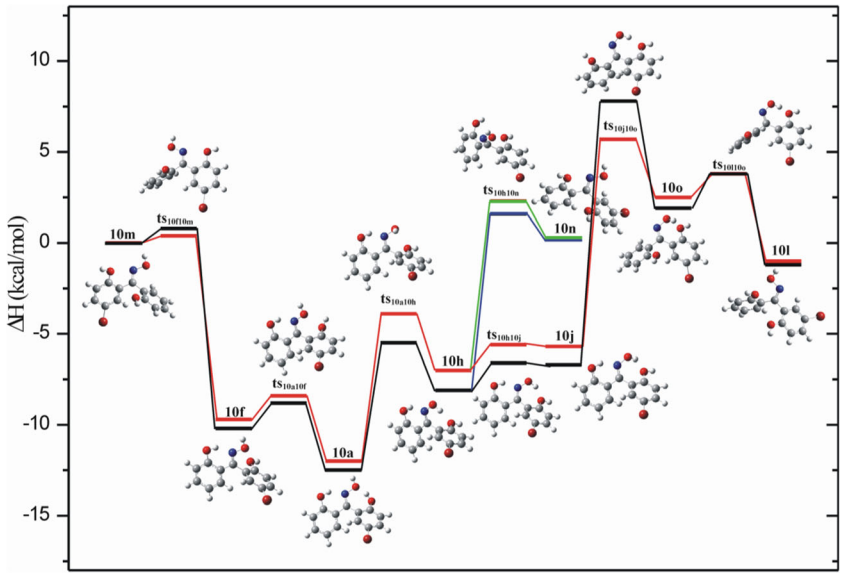

Fig. 10 Reaction enthalpy (298.150 K; 1 Atm) for the conformational isomerization of the open form (type **III**) of **9** and **10** to the closed form (type **I**). *Black lines* correspond to **9** (see Fig. 4) and *red lines* to **10** (see Fig. 4). Only the conformers and transition states of **10** are given for simplicity (C atoms are indicated by *grey spheres*, H by *white*, O by red, N by *blue*, and Br by *dark red*)

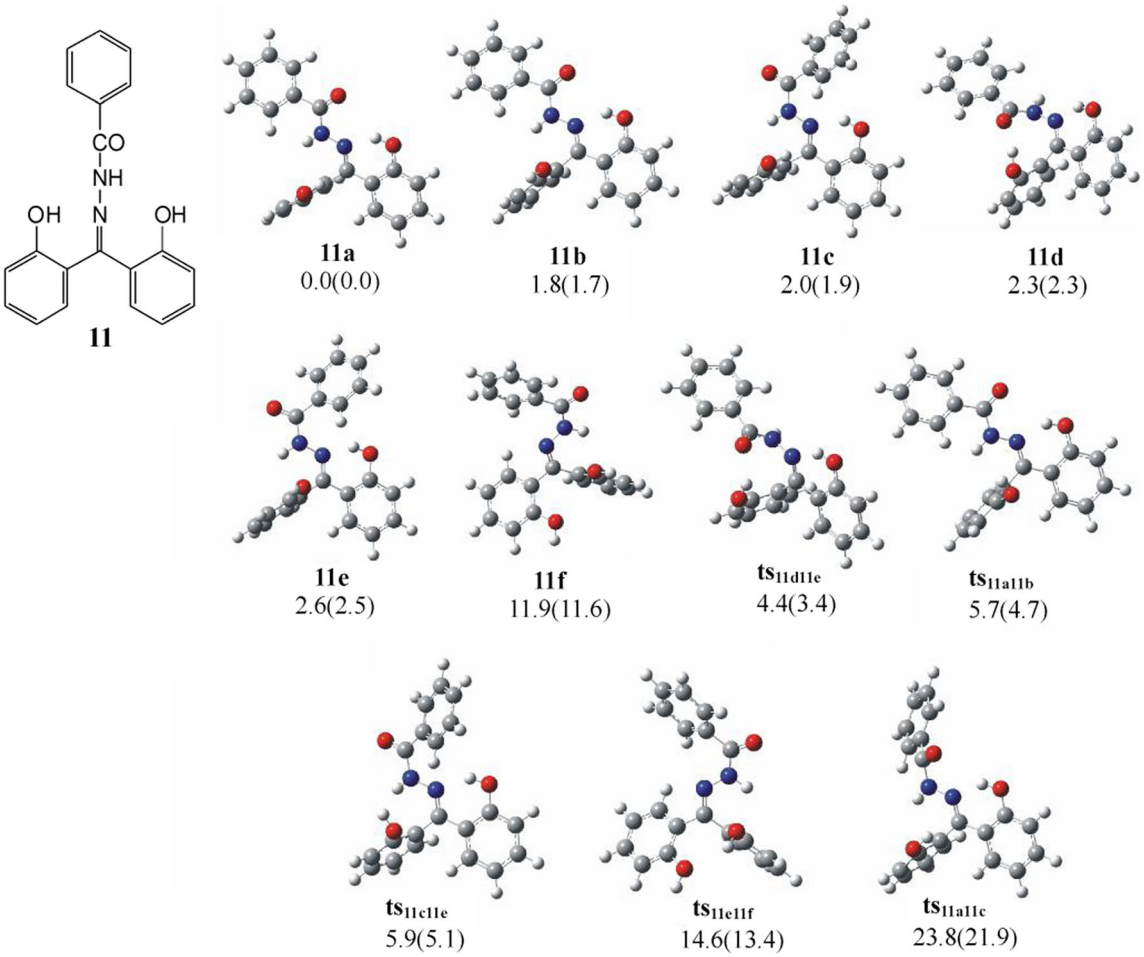

Fig. 11 Minima and transition states (ts) of **11**. The relative energies (relative enthalpies at 298.150 K and 1 Atm) in kcal/mol are given (C atoms are indicated by *grey spheres*, H by *white*, O by *red*, and N by *blue*)

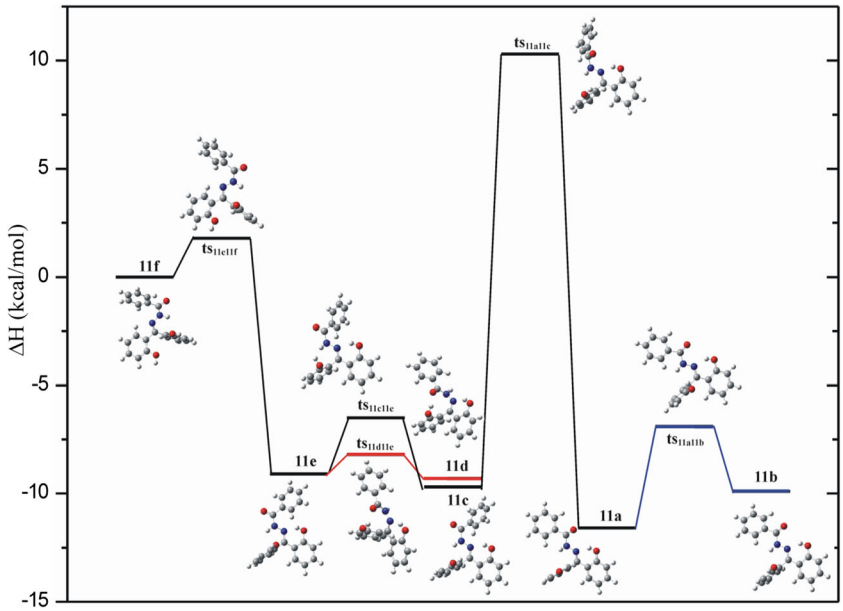

Fig. 12 Reaction enthalpy (298.150 K; 1 Atm) for the conformational isomerization of the open form (type **III**) of **11** to the closed form (type **I**) (C atoms are indicated by *grey spheres*, H by *white*, O by *red*, and N by *blue*)

stabilized pseudo ring [32], in line with the calculated geometry data. Precedents confirm the RAHB-pseudo ring stabilized bridges (bifurcated included) in **1**–**5** [32, 50–53]. Accordingly, not only these bridges affect the inherent reactivity of **1**–**5**, they also protect OH groups. RAHB further deters *o*-oxidation and differentiates the two phenol rings, allowing the synthesis of diverse derivatives [32]. Evidence for the RAHB bridgings has also been obtained from ^{1}H,^{13}C and ^{17}O NMR and FT-IR spectroscopy, 2D NMR data and grid scan analysis [32, 54, 55].

Ether derivatives

6 and **7:** The minima and relative enthalpies of **6** and **7** are shown in Fig. 5. It should be noted that the OH groups are masked/protected (by benzyl moieties), thus, excluding H bonding and pseudo ring formation. The minima of **a** conformer in both structures are similar. Its geometry is not affected by the nature of the *p*-substituent. Interactions between H atoms of phenol rings and the >C=O O atom, most probably of C-H…π type, are detected [25], with bond distances of 2.6–2.7 Å. The $>CH_2$ groups are situated far from the C=O group at the global minima, thus, no CH… π interactions are detected. However, such weak interactions at bond distances of 2.2–2.6 Å are found in the other conformers. The dihedral angles engaging the phenol groups in the lowest minima of **6** and **7** have been estimated (Table 3S, SI).

Oximes

Replacing O by N in the pivotal double bond gives rise to non equivalent H bonding arrangements. Oximes are known to function as H bond donors, through their OH site and acceptors, through their N lone pair [56]. The N and O lone pair repulsion endows the donor-acceptor character to the oxime N and O sites and forces one of the rings out of planarity.

8: The minima and transition states (ts) of the parent **8** are depicted in Fig. 6. The lowest energy minima **8a** and **8e** indicate one six-membered and one seven-membered pseudo rings. The former is built up through the OH H atom (**8a**) whereas the latter engages the H atom from the NOH entity (**8e**). The **8b**, **8c** and **8d** minima form one six-membered pseudo ring, **8h** has one seven-membered pseudo ring while no pseudo rings are found in the **8f** and **8g** (open form) minima. The transition state $\mathbf{ts_{8a8c}}$ between **8a** (closed form) and **8c** (semi-closed form) corresponds to the dismantling of the seven-membered pseudo ring upon rotation of the phenol group, the $\mathbf{ts_{8c8g}}$ transition state between **8c** and **8g** corresponds to the dismantling of the six-membered pseudo ring upon rotation of OH group and the $\mathbf{ts_{8f8g}}$ transition state between **8f** and **8g** (open form) corresponds to the rotation of the oxime OH group. The reaction enthalpy variation for the conformational changes is depicted in Fig. 7. The enthalpy barriers for the **8f** (open) → **8g** (open) → **8c** (semi-closed) → **8a** (closed) conversions are 11.4, 2.0 and 1.4 kcal/mol, respectively.

The intramolecular H bond distances and the O-H… O angles of the six- and seven-membered pseudo rings of the minima and transition states of **8** are given in Table 4S, SI. It should be noted that the RAHB-stabilized six-membered pseudo ring is nearly planar, unlike its seven-membered counterpart. H… O bond distances of 1.8–1.9 Å are longer than those in **1** by

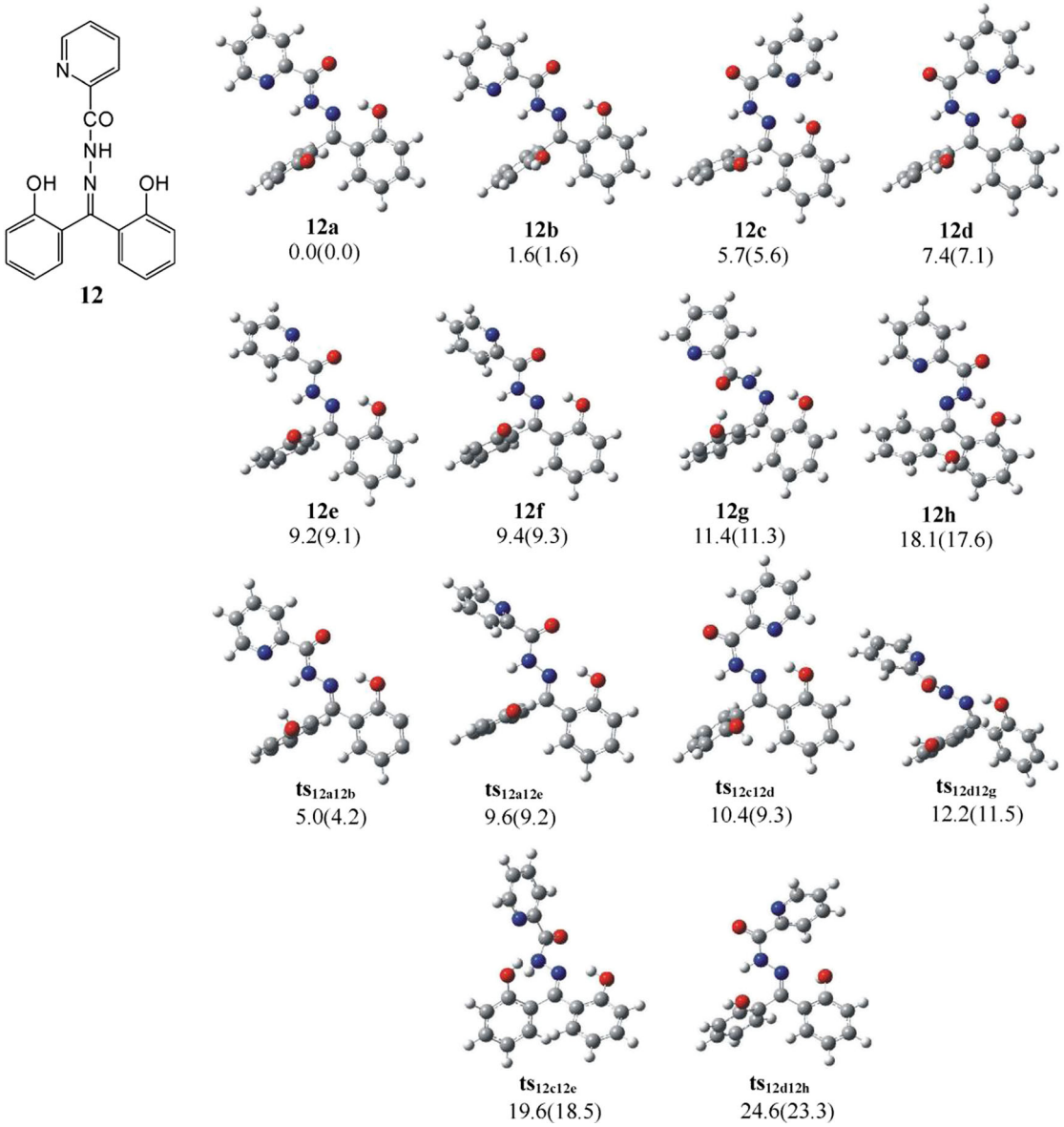

Fig. 13 Minima and transition states (ts) of **12**. The relative energies (relative enthalpies at 298.150 K and 1 Atm) in kcal/mol are given (C atoms are indicated by *grey spheres*, H by *white*, O by *red*, and N by *blue*)

0.15 Å. The H…N bond distance, on the other hand, is expectedly slightly shorter at 1.7–1.8 Å. Their N-O distance, is in agreement with the generally observed range of 2.5–2.6 Å in (aldo)ketoximes [54]. The dihedral angle between the two phenol groups in the lowest energy minimum conformer of **8** is larger to that in **1** by ca. 20 degrees. The NMR data of **8** [32] in contrast to **1**, display the symmetrical protons of the two rings as magnetically non equivalent because of the restricted rotation around the C=N bond of the oxime moiety, which "locks" its OH group in a certain orientation towards one of the two phenol rings, inducing different magnetic environments to their protons in agreement with our calculated geometries.

9 and **10:** The minima and transition states (ts) of **9** and **10** are depicted in Figs. 8 and 9. They both display the same minima and transition states with a nearly identical ordering. All minima are in pairs, e.g. (**a**, **b**) (**c**, **d**) (**e**, **f**) and so on. The paired conformers have identical pseudo ring formations and they only differ to which ring is *p*-substituted. Conformers **a**, **b**, **i**, and **j** each have a six- and a seven-membered pseudo rings; **c** - **h** have one six-membered pseudo ring; **o**, and **p** have one seven-membered pseudo ring; **k**, **l**, **m**, and **n** have no pseudo rings. Transition state $\mathbf{ts_{hj}}$, between **h** and **j** conformers, each having a six-membered ring, carries two pseudo rings. The reaction enthalpy variation for the conversion between the open forms of **l**, **m** and **n** to the closed form **a** are depicted in Fig. 10. The enthalpy barrier for the first step of the

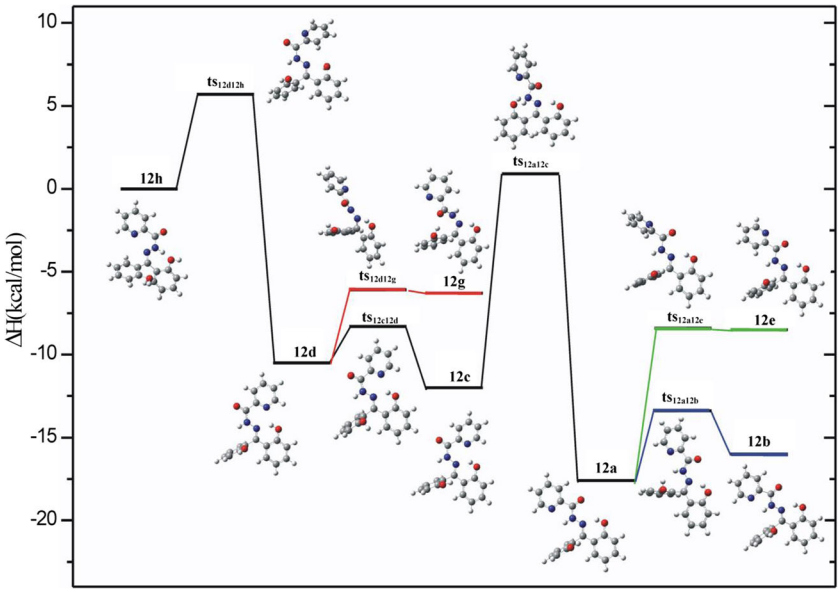

Fig. 14 Reaction enthalpy (298.150 K; 1 Atm) for the conformational isomerization of the open form (type **III**) of **12** to the closed form (type **I**) (C atoms are indicated by *grey spheres*, H by *white*, O by *red*, and N by *blue*)

conformation change **m**, **n**, **l** (open) → **a** (closed) is 1.4(1.3), 2.6(3.1), 5.9(4.8) kcal/mol, respectively. The energy demand for the conformation changes in **10** is slightly lower than that in **9**.

The intramolecular H bond distances and the O-H…O angles of the six- and seven-membered pseudo rings of the minima and transition states of **9** and **10** are given in Table 5S, SI. Comparing the geometries of **8**, **9**, and **10**, we observe that the distances and the angles are similar among the corresponding conformers. Oxime conformers are differentiated by a substitution-triggered symmetry disruption. Thus, bromine substitution in **10**, namely the **10a** and **10b** conformers, is observed in the NMR signals in a population ratio 1:1, indicating the presence of two distinct conformations [32]. Distortions of bonds, their angles and dihedral angles are also in this case indicative of the IHB-stabilized rings. NMR data display symmetrical ring protons as magnetically non equivalent. Grid scan analysis revealed the possibility of H bonding between the phenol OH and the oxime N site.

Hydrazones

Geometry features similar, in part, to those of oximes **8**–**10**, are more pronounced in hydrazones **11**–**13**. The two rings are markedly twisted out of planarity by ca. 60–73 degrees. The extent of the pseudo ring RAHB-driven distortion of the structures is indicated by their dihedral angles sharper to those found in **8**–**10**.

11 and **12:** The minima and transition states (ts) of conformers of **11** are depicted in Fig. 11. The **11a**–**e** conformers form a RAHB-stabilized six-membered pseudo ring while the lowest energy conformer **11d** has a six- and a nine-membered pseudo rings. The latter should be best looked at as a *pseudo* ring-like interaction formed by the pendant N-acyl arm, through a sterically favourable orientation. **11f** has no pseudo rings. The $\mathbf{ts_{11a11b}}$ and $\mathbf{ts_{11c11e}}$ transition states between **11a** and **11b** and between **11c** and **11e**, respectively (all in closed forms) correspond to the rotation of a phenol OH group. The $\mathbf{ts_{11d11e}}$ transition state between **11d** (two pseudo rings) and **11e** (one pseudo ring) corresponds to the dismantling of a nine-membered pseudo ring. The $\mathbf{ts_{11a11c}}$ transition state between **11a** and **11c** (both in closed forms) corresponds to the rotation of NN-CO arm.

We observe that all lowest energy minima lie within a range of 3 kcal/mol. The **11d** minimum, having a six- and a nine-membered pseudo rings, lies only ca. 2.3 kcal/mol above that of **11a** (see Fig. 11). For the conversion process of **11f** (open form) to **11d** (closed form with two pseudo rings) low enthalpy barriers of ca. 1.8 and 1.1 kcal/mol are needed (see Fig. 12). However, for the three-step conversion process of **11f** (open form) to the lowest minimum **11a** a high enthalpy barrier of ca. 20.0 kcal/mol is needed, corresponding to the rotation of NN-CO arm. This transition state lies ca. 10.3 kcal/mol above that of **11f** (open form) while the **11a** lowest minimum lies below that of **11f** by ca. 11.6 kcal/mol. Thus, the required enthalpy barrier is paid by the stabilization enthalpy of the **11f**. The other two steps have limited enthalpy demands of ca. 1.8 and 2.6 kcal/mol, respectively (see Fig. 13). Note that, the energy barrier between $\mathbf{ts_{11a11b}}$ and $\mathbf{ts_{11c11e}}$ transition states for the rotation of the phenol OH group is ca. 3 kcal/mol (see Fig. 12).

The minima of the conformers of **12** are depicted in Fig. 13. In **12** a pyridine has replaced the phenyl ring of **11** as the aryl

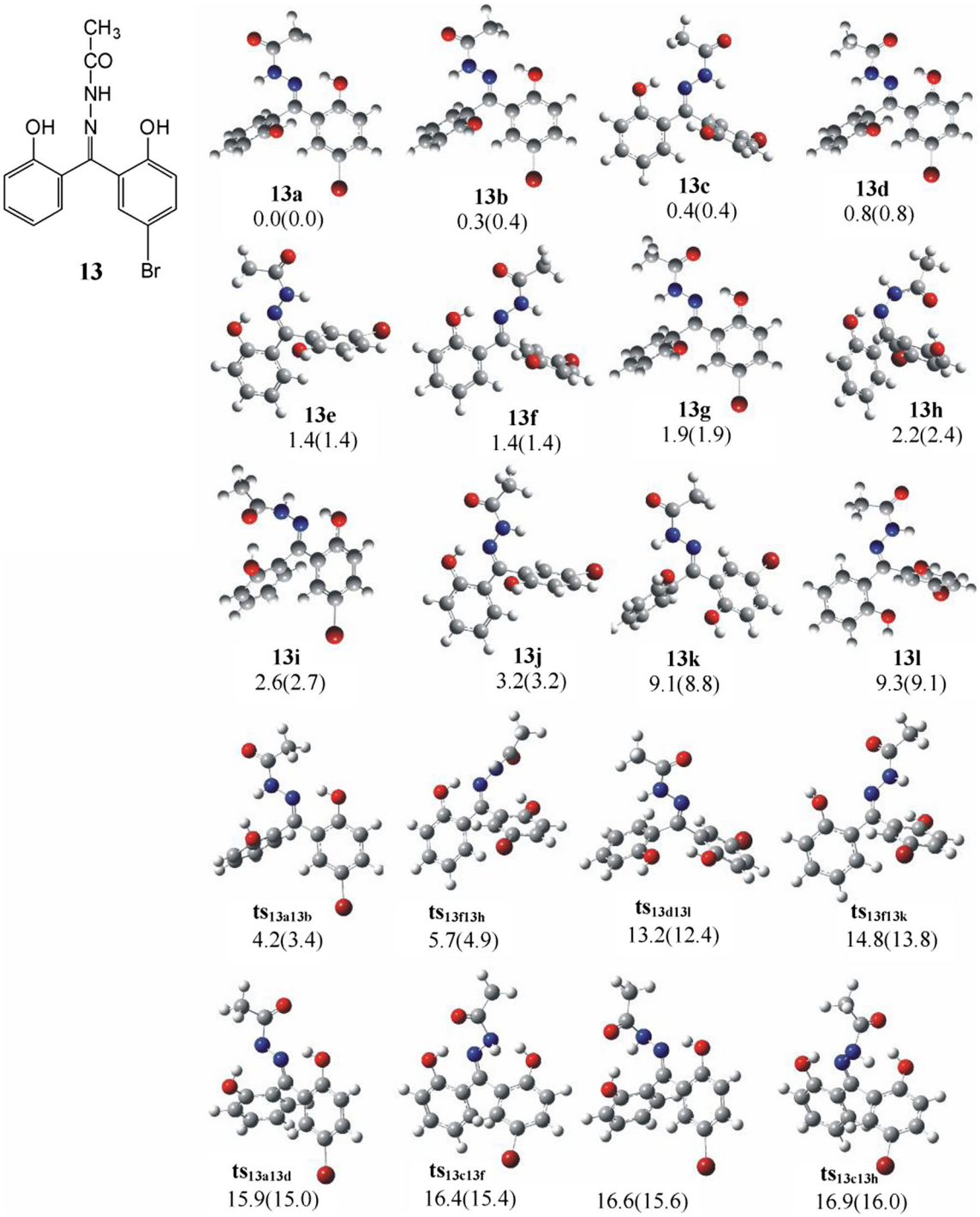

Fig. 15 Minima and transition states (ts) of **13**. The relative energies (relative enthalpies at 298.150 K and 1 Atm) in kcal/mol are given (C atoms are indicated by *grey spheres*, H by *white*, O by *red*, N by *blue*, and Br by *dark red*)

moiety attached to the amide >C=O. All minima have a six-membered pseudo ring except **12g**, which has an additional nine-membered one and **12h** having no pseudo rings. Both **11** and **12** have the same global conformer. However, the existence of the pyridine N atom (through its π electron lone pair) affects the relevant stability of other minima. For example, **11c** and **11e**, resulting from the rotation of the NN-CO arm, lie ca. 2.0 and 2.6 kcal/mol, respectively, above the corresponding **11a** minimum while the corresponding minima of **12c** and **12d** lie ca. 5.7 and 7.4 kcal/mol above the global minimum. The minima with two pseudo rings, i.e. **11d** and **12g**, lie at ca. 2.3 and 11.4 kcal/mol, respectively, above the corresponding

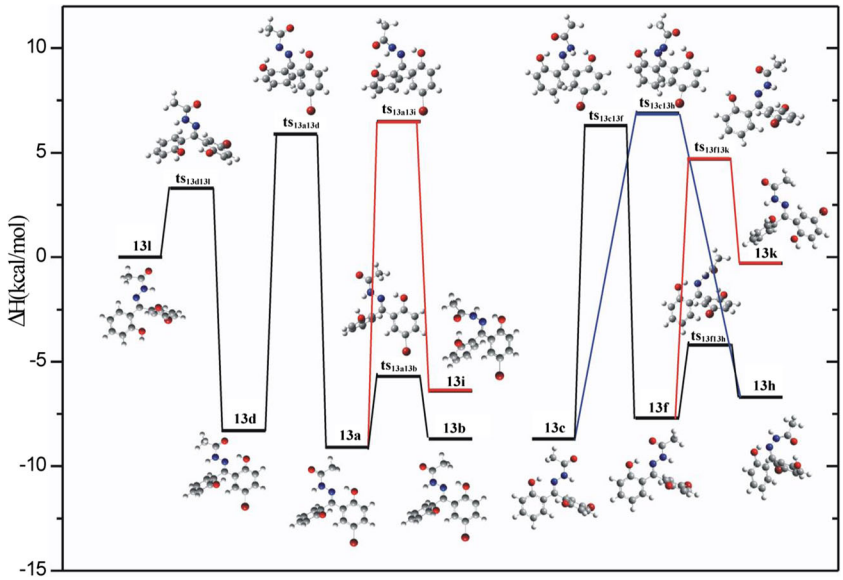

Fig. 16 Reaction enthalpy (298.150 K; 1 Atm) for the conformational isomerization of the open structure (type **III**) of **13** to the closed form (type **I**) (C atoms are indicated by *grey spheres*, H by *white*, O by *red*, N by *blue*, and Br by *dark red*)

global conformer while **11g** and **12h** (open forms) lie at ca. 11.9 and 18.1 kcal/mol. Overall, the pyridine σ and π geometry increases the separation of the various minima, compared with those with the phenyl ring. **12a**, **12e**, and **12f** differ only with respect to the relative orientation of pyridine ring. The transition states of **12** are depicted in Fig. 13. Worth noting is that transition states of **11** and **12** are similar between **a** and **b** only, i.e., $\mathbf{ts_{11a11b}}$ and $\mathbf{ts_{12a12b}}$ whereas notable differences are detected among the rest.

The reaction enthalpy variation for the conversion between **12h** (open form) to the lowest energy minimum **12a** (with one pseudo ring) and to **12g** (with two pseudo rings) is depicted in Fig. 14. Comparing the enthalpy variation for the conversion processes in **11** (Fig. 12) and **12** (Fig. 14) we observe the following notable changes, (a) the first step in **12** has a barrier of ca. 5.7 kcal/mol compared with that of ca. 1.8 kcal/mol for **11**, (b) a demanding barrier of ca. 20 kcal/mol between the **c** and **a** conformers of **11** is diminished to 12.9 kcal/mol for **12**, (c) The OH rotation barrier between **a** and **b** or **c** and **d** is ca. 2.5 kcal/mol and (d) the barrier from **12d** to **12g** (minima with two rings) is ca. 4.3 kcal/mol.

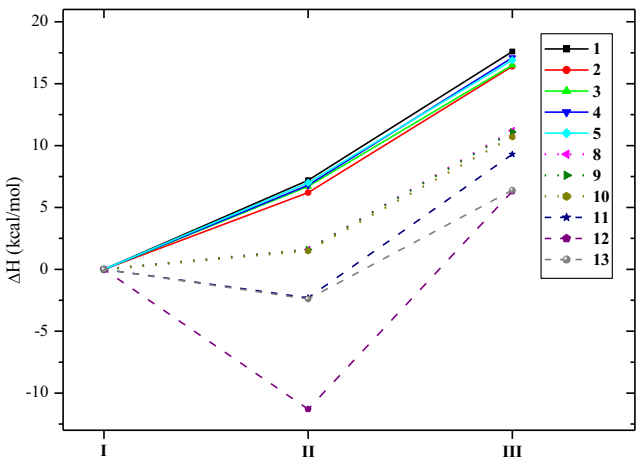

Fig. 17 Relative enthalpies (298.150 K; 1 Atm) of the lowest energy conformers of types **I**, **II**, and **III**

The intramolecular H bond distances and the O-H…O and O-H…N angles of the six- seven- and nine-membered pseudo rings and the dihedral angles of the minima and transition states of **11** and 12 are given in Table 6S, SI. The corresponding H…N bond distance is ca. 1.7–1.8 Å whereas the H…O distance in the nine-membered ring is ca. 1.813 (**11d**), 1.823 (**12g**), and 2.047 for $\mathbf{ts_{11d11e}}$. The six-membered pseudo ring-forming H atom interacts with the pyridine N atom in **12c**, **12d**, and $\mathbf{ts_{12c12d}}$ having a H… N distance of ca. 2.2 Å. The lowest energy minimum dihedral angle between the two phenol groups is 80 degrees in both **11** and **12**, i.e. larger by 17 degrees to that of oxime **8** and 37 degrees to that of parent ketone **1** (see Tables 1S, 4S and 6S of SI). A H…N distance of ca. 1.944 Å is found in the $\mathbf{ts_{12a12c}}$ transition state, having an additional seven-membered ring, ca. 0.2 Å longer than the H…N distances of the six-membered pseudo rings (see Fig. 14). Further, the dihedral angles between the phenyl (in **11**) or pyridine (in **12**) groups and the phenol closer to either, of 68.0 degrees vs 3.6 degrees, indicate and reflect a strong impact of the pyridine ring in the adopted conformation. NMR data and grid scan analysis for **11** and **12** reveals the possibility of H bonding between the phenol OH and the hydrazone N site [32]. The results are in agreement with the present DFT

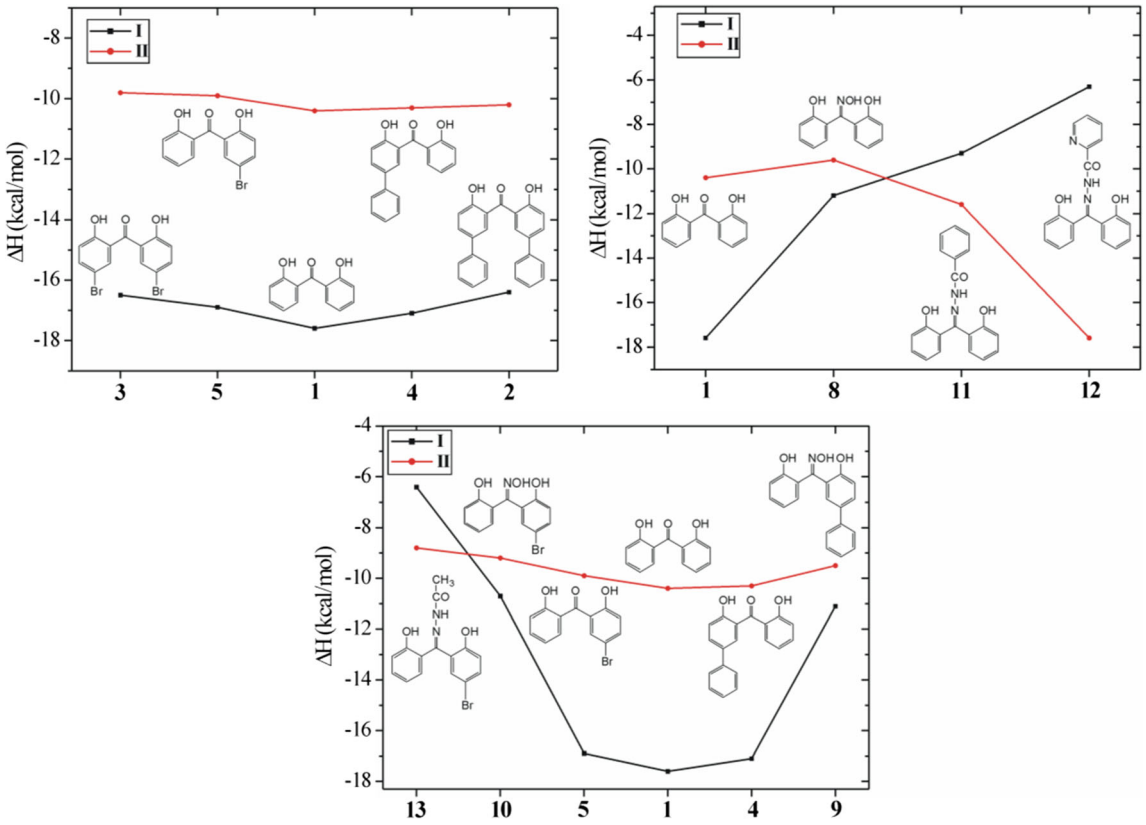

Fig. 18 Variation of the formation enthalpy of the lowest in energy conformer of types **I** and **II** from **III**

calculations, confirming the formation of a six-membered pseudo ring.

13: Minima and transition states (ts) of **13** are depicted in Fig. 15. All minima, except **13h** and **13i**, have only one six-membered pseudo ring. **13h** and **13i** have an additional nine-membered pseudo ring, while **13k** and **13l** have no pseudo rings. Note that **13a** (conformer carrying the *p*-Br substituent in one of the phenol rings) and **13c** (conformer carrying the unsubstituted phenol ring) give different minima for the six-membered pseudo ring formation. Comparing energetically the conformers of **13** with those of **11** and **12**, we observe that the minima in **13** exhibit smaller relative energy differences than in **11** or **12**. For example, **a** and **b** forms in **11**–**13** differ in the O-H bond orientation with energy differences of 1.8, 1.6 and 0.36 kcal/mol for **11**, **12** and **13**, respectively. The $\mathbf{ts_{13a13b}}$ transition state corresponds to a barrier of OH rotation, $\mathbf{ts_{13a13d}}$ and $\mathbf{ts_{13c13f}}$ correspond to a barrier of NN-CO rotation, $\mathbf{ts_{13d13l}}$ and $\mathbf{ts_{13f13k}}$ correspond to a barrier for the formation of a six-membered pseudo ring, $\mathbf{ts_{13f13h}}$ $\mathbf{ts_{13a13i}}$, and $\mathbf{ts_{13c13h}}$ correspond to a barrier for the formation of an additional nine-membered pseudo ring. The reaction enthalpy variation for the conformational changes between the open forms of **13k** or **13l** to the lowest energy minima of **13a** or **13c** with one pseudo ring and to **13d** with two pseudo rings, is depicted in Fig. 16. It is interesting that the $\mathbf{ts_{13d13l}}$ is stabilized via an eight-membered pseudo ring and the $\mathbf{ts_{13a13d}}$ and $\mathbf{ts_{13c13f}}$ are stabilized via a seven-membered pseudo ring (see Fig. 16).

The intramolecular H bond distances, the O-H… O and O-H…N angles of the six-, seven-, eight- and nine-membered pseudo rings and the dihedral angles of the minima and transition states of **13** are given in Table 7S, SI. An intramolecular H…N bond distance of ca. 1.7–1.8 Å and a H…O distance of the nine-membered ring of ca. 1.83 Å and 2.0–2.4 Å at the transition states have been estimated. The dihedral angle between the two phenol rings in the lowest energy minimum is 100 degrees, i.e. ca. 20 degrees larger than the corresponding one in **11** and **12** (see Tables 6S and 7S, SI). The $\mathbf{ts_{13a13d}}$ and $\mathbf{ts_{13c13f}}$ transition states with an additional seven-membered ring (see Fig. 14) display H…N distances of ca. 1.90 Å, i.e. ca. 0.2 Å longer than the H…N distances of the six-membered pseudo rings. On the other hand, an eight-membered ring is formed by the interaction of two OH groups, having H…O distances of ca. 2.1 Å (see Fig. 15).

The two rings are markedly twisted out of planarity by ca. 60–73 degrees [32, 57]. **11**–**13** display their symmetrical phenol ring protons as magnetically non equivalent [32]. The intramolecular H bonding is probed by the deshielded ^{1}H NMR resonances in the range 10.5–13.2 ppm supported by grid scan analysis.

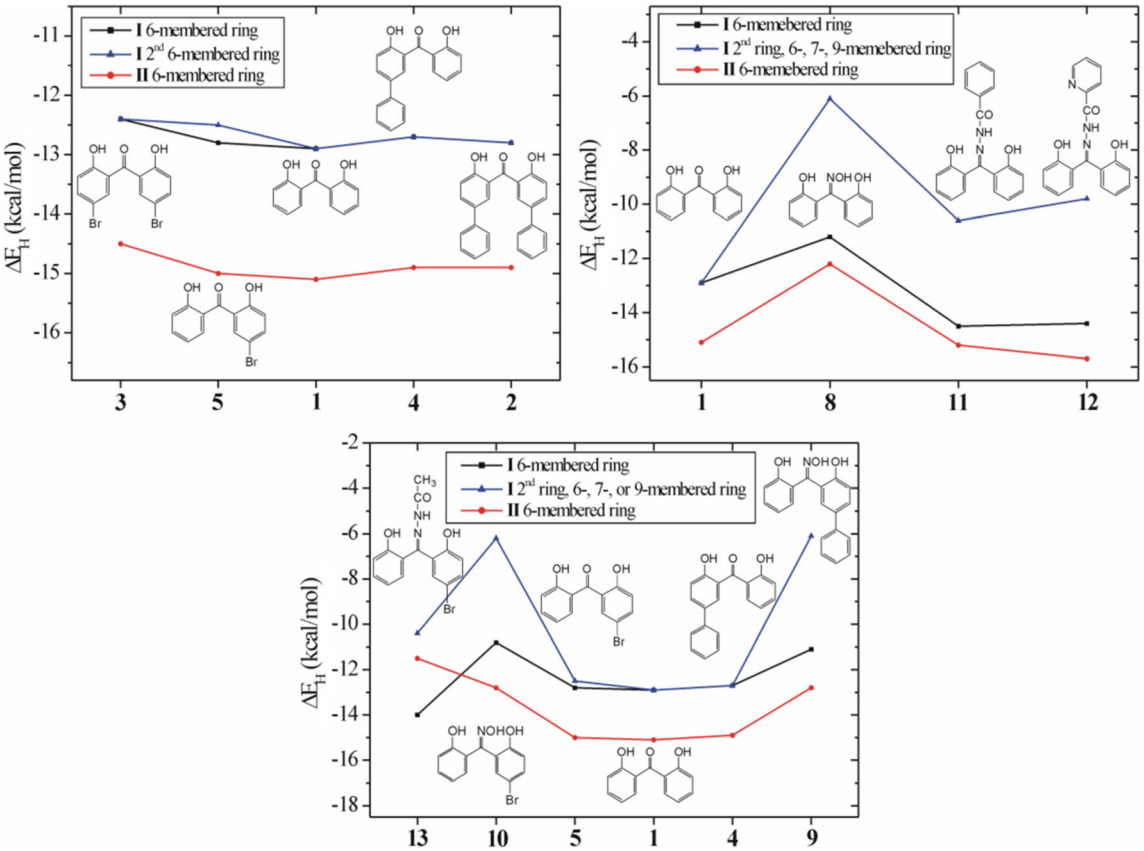

Fig. 19 Variation of the intramolecular H bond energy of the lowest energy conformer of types **I** and **II**

Impact of intramolecular H bonding on conformation

The effects of intramolecular H bonding (IHB) on the lowest energy conformers of types **I** and **II** are discussed in terms of (a) relative formation enthalpies and (b) dipole moments of compounds **1**–**13**, modified by *p*-substitution (see Figs. 17, 18, 19, 20, and 21), bearing in mind that a H bond is considered as a deprotonation event or an arrested intermediate in an acid-base equilibrium [25]. Observed variations display the significance of IHB as a major determinant of favoured conformations.

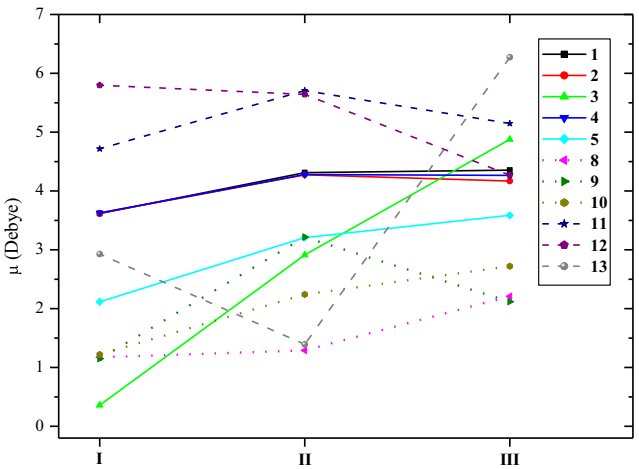

Fig. 20 Dipole moments μ of the lowest energy conformer of types **I**, **II**, and **III**

Relative enthalpies of the lowest energy conformers of types **I**, **II**, and **III** in **1**–**5** and **8**–**13** are shown in Fig. 17. These exhibit similar trends in ketones **1**–**5** and oximes **8**–**10** but not in hydrazones **11**–**13**. The largest enthalpy of stabilization is found in type **I** conformers compared to those of type **III**, being 17.6 and 11.2 kcal/mol for the parent members **1** and **8**, respectively, among **1**–**10** (see Fig. 17). Most stable in **11**–**13**, relative to type **III**, are the type **II** conformers, estimated as 17.6 kcal/mol (**12**), 11.6 kcal/mol (**11**), and 8.8 kcal/mol (**13**). Energy demands of like magnitude are shown in **12** and **13** type **I** conformers and it is **11** that appears to be somewhat less demanding by ca. 3 kcal/mol. Similar trends are obtained for the Gibbs free energies (see Fig. 1S, SI). An overall decrease is observed in the enthalpy of formation of **1**–**10** for both types **I** and **II**, in contrast with a reverse trend noted in type **II** hydrazones **11** and **12**. Enthalpy

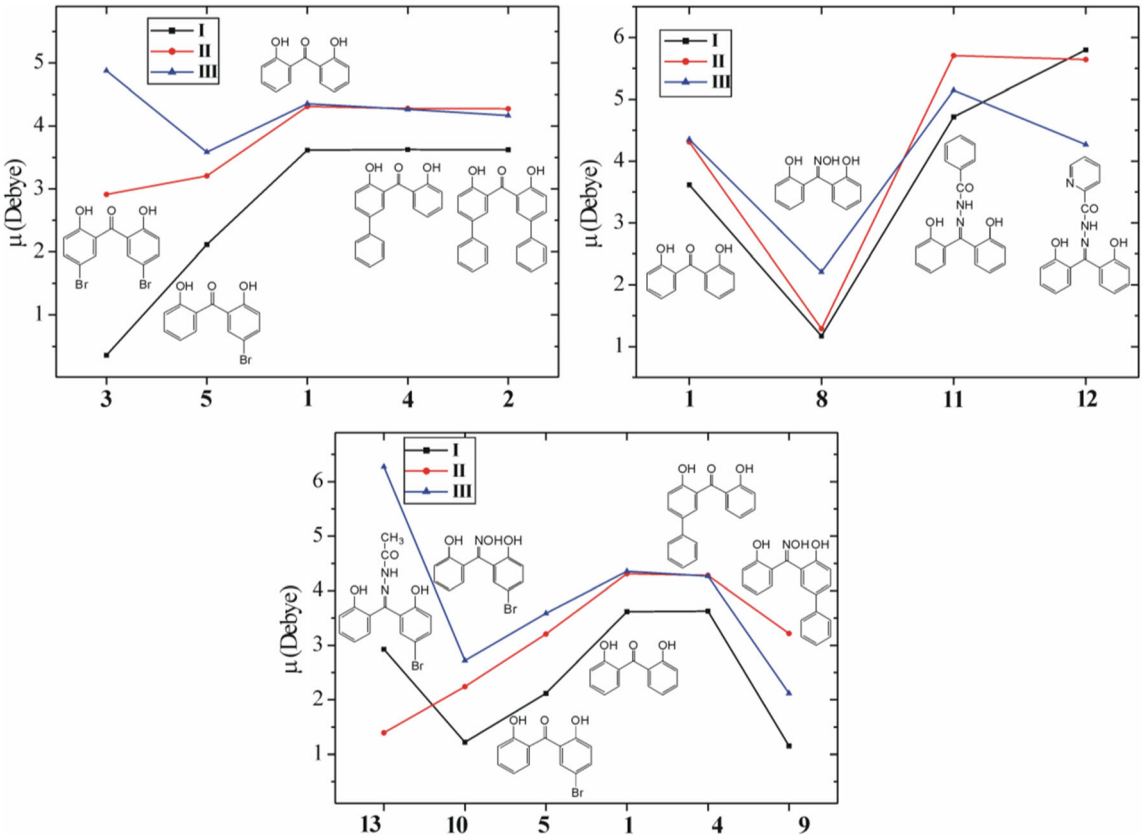

Fig. 21 Variation of the dipole moments μ of the lowest energy conformer of types **I**, **II**, and **III**

changes for the lowest energy conformers of types **I** and **II** against those of type **III** are shown in Fig. 18.

The IHB energy (E_H) in type **I** and **II** of the series as well as its sum of type **I** (two IHBs, i.e. two pseudo rings) (E_{2H}) are given in Table 8S, SI. These values correspond to the energy required for the O-H rotation by a steering angle of 180 degrees [58]. In ketones **1**–**5** we observe H bond energies of ca. -13 kcal/mol for each H bond of the bifurcation domain of type **I** conformers and ca. -15 kcal/mol for type **II** conformers. Expectedly lower energies than those in **1**–**5** by ca. 2 kcal/mol (i.e. ca. -11 kcal/mol for type **I** and ca. -13 kcal/mol for the type **II′** conformers) are found for the OH…N H bonds, building up the six-membered rings, in oximes **8**–**10**. The energy of that bond, corresponding to the 2nd seven-membered ring, is further lowered to ca. 6 kcal/mol for type **I** and only ca. -0.3 kcal/mol for type **II″**. This decrease is clearly attributed to the larger size and much greater distortion of the latter ring. The energy of the OH… N bond of six-membered ring in hydrazones, is 12–16 kcal/mol for the types **II** and **I** while the corresponding one for the nine-membered ring is ca. 10 kcal/mol.

Enthalpies of IHB formation for the lowest energy conformers of types **I** and **II** shown in Fig. 19. A marginal decrease in **1**–**5**, a further significant drop in **8**–**10** and a reverse of this trend in **11**–**13** (except in type **II** conformers of **13**) are observed, traited to *p*-substitution steric pleas.

Dipole moments (μ) of the lowest energy type **I**-**III** conformers, shown in Fig. 20, in agreement with the already discussed data indicate an expectedly substantial sensitivity of polarity to conformation, clearly implicating the IHB interactions. Accordingly, apart from ketones **1**, **2** and **4**, having a μ = 4D, in any conformation, all other conformations in **1**–**13** exhibit dramatically varying μ values, for instance 0.4D (type **I**), 2.9D (type **II**), and 4.9D (type **III**) for **3** and 2.9D (type **I**), 1.4D (type **II**) and 6.3D (type **III**) for **13**. The highest values are observed in hydrazones **11**–**13**. Dipole changes for the lowest energy conformers of types **I** and **II** against those of type **III** are shown in Fig. 21.

Conclusions

The lowest energy conformer in ketones **1**–**5** has a homomeric bifurcation bridge (i.e two six-membered pseudo rings), a heteromeric bifurcation bridge (i.e. one six- and one seven-membered pseudo rings) in oximes **8**–**10** while that in **11**–**13** has only one six-membered pseudo ring. H-bonded (singly and bifurcated) conformations are expectedly more stable than their non H-bonded congeners throughout the series **1**–**13**. This is clearly more notable in **1**–**5** than **8**–**10**, particularly so for their parent members **1** and **8**, as revealed by enthalpy changes of ca. 17 and 11 kcal/mol, respectively or barriers of

ca. 3 kcal/mol. Corresponding H-bonded conformers against their non H-bonded ones in **11**–**13** series, on the other hand, reveal no trends, stability of H-bonded conformers comparable to that in **1**–**5** or **8**–**10** and greater energy demands for conformation interconversions. Enthalpy and interconversion barrier data as well as dipole moments among the various conformations demonstrate (a) stabilization infused by intramolecular H bonding, (b) additional stabilization endowed by bifurcation, particularly a homomeric bridging one, (c) the greater enthalpy demands in O-based H-bonded rings and (d) a weaker stabilization of a N-engaging H bridge compared to an O atom one, reflecting their relative nucleophilicities.

References

1. Baughan BM, Stennett E, Lipner RE, Rudanwsky AC, Schmidke SJ (2009) J Phys Chem A 113:8011–8019
2. Kumasaka R, Kikuchi A, Yagi M (2014) Photochem Photobiol 90:727–733
3. Momekov G, Nedialkov PT, Kitanov GM, Zheleva-Dimitrova DZ, Tzanova T, Girreser U, Karaivanova M (2006) Med Chem 2:377–384
4. Catalán J, De Paz JLG, del Valle JC, Kasha M (1997) J Phys Chem A 101:5284–5291
5. Keck J, Roessler M, Schroeder C, Stueber GJ, Waiblinger F, Stein M, LeGourriérec D, Kramer HEA, Hoier H, Henkel S, Fischer P, Port H, Hirsch T, Rytz G, Hayoz P (1998) J Phys Chem B 102:6975–6985
6. Nguyen LH, Venkatraman G, Sim KY, Harrison LJ (2005) Phytochemistry 37:1718–1723
7. Ignasiak MT, Levin CH, Kciuk G, Marciniak B, Pedzinski T (2015) Chem Phys Chem 16:628–633
8. Suzuki T, Kitamura S, Khota R, Sugihara K, Fujimoto N, Ohta S (2005) Toxicol Appl Pharmacol 203:9–17
9. Padrón AJC, Aguirre G (1989) Eur Polym J 25:25–29
10. Hagedorn-Leweke U, Lippold BC (1995) Pharmacol Res 12: 1354–1360
11. Martin R (2011) Aromatic Hydroxyketones: Preparation and Physical Properties, 3rd ed, Springer. 1
12. Romão MJ, Knäblein J, Huber R, Moura JJG (1997) Prog Biophys Mol Biol 68:121–144
13. Minutolo F, Bertini S, Martinelli A, Ortore G, Placanica G, Prota G, Rapposelli S, Tuccinardi T, Sheng S, Carlson KE, Katzenellenbogen BS, Katzenellenbogen JA, Macchia M (2006) ARKIVOC 8:83–94 **and references cited therein**
14. Ley JP, Bertram HJ (2001) Bioorg Med Chem 9:1879–1885
15. Rollas S, Küçükgüzel SG (2007) Molecules 12:1910–1939
16. Verma G, Marella A, Shaquiquzzaman M, Akhtar M, Ali MR, Alam MM (2014) J Pharm Bioallied Sci 6:69–80
17. Khanum SA, Girish V, Suparshwa SS, Khanum NF (2009) Bioorg Med Chem Lett 19:1887–1891
18. Zahedi-Tabrizi M, Tayyari SF, Badalkhani-Kamseh F, Ghomi R, Afshar-Qahremani F (2014) J Chem Sci 126:919–929
19. Xu X, Cao Z, Zang Q, Zhang Q (2005) J Chem Phys 122:194305
20. Madsen GKH, Iversen BB, Larsen FK, Kapon M, Reisner GM, Herbstein FH (1998) J Am Chem Soc 120:1004–10045
21. Lenain P, Mandado M, Mosquera RA, Bultinck P (2008) J Phys Chem A 112:10689–10696
22. Beck JF, Mo Y (2007) J Comput Chem 28:455–466
23. Feldblum ES, Arkin IT (2014) PNAS 111:4085–4090
24. Martínez-Cifuentes M, Weiss-López BE, Santos LS, Araya-Maturana R (2014) Molecules 19:9354–9368
25. Pairas GN, Tsoungas PG (2016) ChemistrySelect 1:4520–4532
26. Krygowski T.M., Zachara-Horeglad J.E., Paluciak M., J Org Chem, 2010, 75, 4944-4949; Gilli G, Bellucci F, Ferretti V, Bertolasi V (1989) J Am Chem Soc 111:1023–1028
27. Tuckerman ME, Marx D, Klein ML, Parrinello M (1997) Science 275:817–820
28. Jeffrey GA (1997) An Introduction to Hydrogen Bonding. Oxford University Press, New York, Oxford
29. Ballesteros JA, Deupi X, Olivella M, Haaksma EE, Pardo L (2000) Biophys J 79(5):2754–2760
30. Shapovalov MV, Dunbrack Jr RL (2011) Structure 19(6):844–858
31. Gardikis Y, Tsoungas PG, Potamitis C, Zervou M, Cordopatis P (2011) Heterocycles 83:1077–1091 **and 1291-1302**
32. Tzeli D, Kozielewicz P, Zervou M, Potamitis C, Kokkotou K, Rak B, Petrou A, Tsolaki E, Gavalas A, Geronikaki A, Petsalakis ID, Tsoungas PG (2016) Chem Select 1:2426–2438
33. Seo MS, Kim K, Kim H (2008) Angew Chem Int Ed 47:8657–8660 **(2013) Chem Commun 49:11623-11625**
34. Perperopoulou FD, Tsoungas PG, Thireou TN, Rinotas VE, Douni EK, Eliopoulos EE, Labrou NE, Clonis YD (2014) Bioorg Med Chem 22:3957–3970
35. Becke AD (1993) J Chem Phys 98:1372–1377
36. Lee C, Yang W, Parr RG (1988) Phys Rev B 37:785–789
37. Curtiss LA, McGrath MP, Blandeau J-P, Davis NE, Binning Jr RC, Radom L (1995) J Chem Phys 103:6104–6113
38. Zhang J-P, Zhou X, Bai FQ, Zhang HX, Tang AC (2009) Theor Chem Accounts 122:31–42
39. Wang H, Meng F (2010) Theor Chem Accounts 127:561–571
40. Irfan A, Zhang J-P, Chang YF (2010) Theor Chem Accounts 127: 587–594
41. Tzeli D, Petsalakis ID, Theodorakopoulos G (2011) Phys Chem Chem Phys 13:954–965
42. Simón L, Goodman JM (2011) Org Biomol Chem 9:689–700
43. Tzeli D, Tsoungas PG, Petsalakis ID, Kozielewicz P, Zloh M (2015) Tetrahedron 71:359–369
44. Gaussian 09, Frisch MJ, Trucks GW, Schlegel HB, Scuseria GE, Robb MA, Cheeseman JR, Scalmani G, Barone V, Mennucci B, Petersson GA, Nakatsuji H, Caricato M, Li X, Hratchian HP, Izmaylov AF, Bloino J, Zheng G, Sonnenberg JL, Hada M, Ehara M, Toyota K, Fukuda R, Hasegawa J, Ishida M, Nakajima T, Honda Y, Kitao O, Nakai H, Vreven T, Montgomery JA, Jr, Peralta JE, Ogliaro F, Bearpark M, Heyd JJ, Brothers E, Kudin KN, Staroverov VN, Kobayashi R, Normand J, Raghavachari K, Rendell A, Burant JC, Iyengar SS, Tomasi J, Cossi M, Rega N, Millam JM, Klene M, Knox JE, Cross JB, Bakken V, Adamo C, Jaramillo J, Gomperts R, Stratmann RE, Yazyev O, Austin AJ, Cammi R, Pomelli C, Ochterski JW, Martin RL, Morokuma K, Zakrzewski VG, Voth GA, Salvador P, Dannenberg JJ, Dapprich S, Daniels AD, Farkas Ö, Foresman JB, Ortiz JV, Cioslowski J, Fox DJ (2009) Gaussian, Inc., Wallingford
45. Gilli G, Gilli P in *The Nature of the Hydrogen Bond: Outline of a Comprehensive Hydrogen Bond Theory*, Oxford scholarship Monographs (2009)
46. Cox PJ, Kechagias D, Nelly O (2008) Acta Cryst B64:206–216
47. Schlemper EO (1982) Acta Cryst B38:1619–1622 **and references cited therein**
48. Landre IMR, Martins FT, Ellena JA, Dos Santos MH, Doriguetto AC (2012) Acta Cryst C68:156–159
49. Jaccard G, Lauterwein J (1986) Helv Chim Acta 69:1469–1485
50. Kuhn B, Mohr P, Stahl M (2010) J Med Chem 53:2601–2611
51. Andersen KB, Langgard M, Spanget-Larsen J (1999) J Mol Struct 509:153–163
52. Lu L, He L (2012) J Mol Struct 1010:79–84
53. Parra RD, Streu K (2011) Comput Theor Chem 977:181–187

54. Smith AG, Tasker PA, White DJ (2003) Coord Chem Reviews 241: 61–85
55. Bondi A (1964) J Phys Chem 68:441–451
56. Politzer P, Murray JS in *The Chemistry of Functional Groups*, Patai series, ed. Rappoport Z, Liebman JE, Chapters 1and 3 (2009) Wiley Interscience
57. Jabeen I, Pleban K, Rinner U, Chiba P, Ecker GF (2012) J Med Chem 55:3261–3278
58. Nowroozi A, Hajiabadi H (2014) Struct Chem 25:215–220